Ground states and the critical behavior in the quasi-one-dimensional complexes $(TMTTF)_2[(AsF_6)_x(SbF_6)_{1-x}]$

F. Iwase,[1,*] K. Sugiura,[2] K. Furukawa,[1,2] and T. Nakamura[1,2]
[1]*Institute for Molecular Science, Myodaiji, Okazaki 444-8585, Japan*
[2]*The Graduate University for Advanced Studies, Myodaiji, Okazaki 444-8585, Japan*
(Received 17 February 2010; revised manuscript received 14 June 2010; published 25 June 2010)

^{13}C NMR measurements were carried out to understand the chemical pressure effect on the ground state in quasi-one-dimensional (1D) organic complexes using the alloy system $(TMTTF)_2[(AsF_6)_x(SbF_6)_{1-x}]$ $(x\sim 0.3, 0.5, 0.67)$. The temperature of the charge-ordering transition decreases with the concentration of AsF_6. Additional line splitting and the rapid increase in the spin-lattice relaxation rate, $1/T_1$, on cooling for the salt of $x\sim 0.3$ indicates that the ground state of the salt is antiferromagnetic. In the $x\sim 0.67$ alloy, the spin gap opens without antiferromagnetic spin correlations. The intermediate salt of $x\sim 0.5$ is located in the vicinity of the quantum critical region between two phases at low temperatures. The quasi-1D correlation and antiferromagnetic critical behavior are discussed in terms of the power-law behavior of $1/T_1$.

DOI: 10.1103/PhysRevB.81.245126 PACS number(s): 71.20.Rv, 71.30.+h, 71.45.Lr, 76.60.−k

I. INTRODUCTION

There is a wide range of physical phenomena in low-dimensional organic conductors, because of the large variety of molecular structures and the effects of strong electron correlation and/or electron-lattice coupling, which are easily modulated by temperature and pressure. Various phase transitions such as the metal-insulator transition, superconductivity, and relevant magnetic phase transitions in low-dimensional electron systems are especially important contemporary issues in condensed-matter physics.[1,2] In one-dimensional (1D) systems, the Fermi-liquid model of Landau, which predicts the behavior of physical properties of metals, is violated due to quantum fluctuations in addition to strong electron correlation.[3] In charge-transfer organics, the anisotropic π orbital in molecules forms the configuration for low-dimensional electron transfer. Weak three dimensionality is introduced by interchain and interlayer couplings, whose contributions induce various phase transitions.

The family of quasi-one-dimensional $(TMTTF)_2X$, where TMTTF is tetramethyltetrathiafulvalene, shows various ground states, including antiferromagnetic, spin gap (spin Peierls), and superconductivity, based on the substitution of X $[X=TaF_6, SbF_6, AsF_6, PF_6, Br, \ldots]$.[1,4] $(TMTTF)_2SbF_6$ is located on the negative pressure side of the generalized phase diagram proposed in Refs. 1 and 5 and undergoes an antiferromagnetic phase transition at $T_N\sim 8$ K.[6,7] The substitution of the anion SbF_6 to AsF_6 works as chemical pressure, leading to the nonmagnetic spin-gapped ground state below $T_{SG}=14$ K.[8–10] This phase transition has been identified to be the spin-Peierls transition for a one-dimensional system. However, the interchain interaction has considerable contribution to the phase transition in the TMTTF system. The thermal-expansion measurement shows that the interchain distance is strongly affected at the transition.[11]

The TMTTF family shows a metal-to-insulator crossover by lowering the temperature. The characteristic crossover temperature is denoted by T_ρ, below which $d\rho/dT$ becomes negative, where ρ is the conductivity. The T_ρ for $(TMTTF)_2SbF_6$ and $(TMTTF)_2AsF_6$ are roughly 150 K and 140 K, respectively.[5,12–14] In the insulator phase, most salts undergo charge ordering (CO), wherein the charges are localized at alternate sites along the chain by the strong long-range electron correlation.[15] The transition temperature, T_{CO}, tends to decrease with pressure, which increases the electron transfer along the chain and reduces the degree of dimerization of TMTTF molecules in the unit cell.[16,17] T_{CO} of $(TMTTF)_2SbF_6$ and AsF_6 are about 155 K and 100 K, respectively.[9,16,18,19]

In general, if two second-order phase transitions share a boundary at absolute 0 K in the pressure-temperature (P-T) phase diagram, there is a characteristic region, the so-called quantum critical region, at low temperatures. Quantum critical physics has attracted significant recent attention with respect to the mechanism of high-T_c superconductivity and non-Fermi-liquid behavior in heavy fermions.[20–24] In the TMTTF system, since the difference in the chemical pressure between SbF_6 and AsF_6 salts is less than 10 kbar, considering the pressure dependence of T_{CO},[5] the existence of a phase boundary is expected in the narrow pressure region. The alloy system $(TMTTF)_2[(AsF_6)_x(SbF_6)_{1-x}]$ is a promising candidate for investigating the properties of ground states and the phase boundary between antiferromagnetic and spin-gap phases.[25,26] Previous experiments using electron spin resonance (ESR) and magnetic susceptibility have detected the antiferromagnetic phase transition and the spin-gap transition near the pure compounds SbF_6 and AsF_6 salt, respectively.[10,25,26] The pressure-temperature phase diagram shows a decrease in the Néel temperature and the spin-gap transition temperature toward the middle pressure range. Conductivity measurements indicate that T_c, defined as the temperature at which the value of $d[\ln\rho]/d(1/T)$ shows a maximum, decreases with the concentration of AsF_6.[12] There is no information available about the concentration dependence of the behavior of charge ordering and the ground-state property near the phase boundary in this system.

In this paper, we report a ^{13}C NMR study of the ground states and critical behavior in the alloy system $(TMTTF)_2[(AsF_6)_x(SbF_6)_{1-x}]$ $(x\sim 0.3, 0.5, 0.67)$. The ground state varies depending on the concentration. The an-

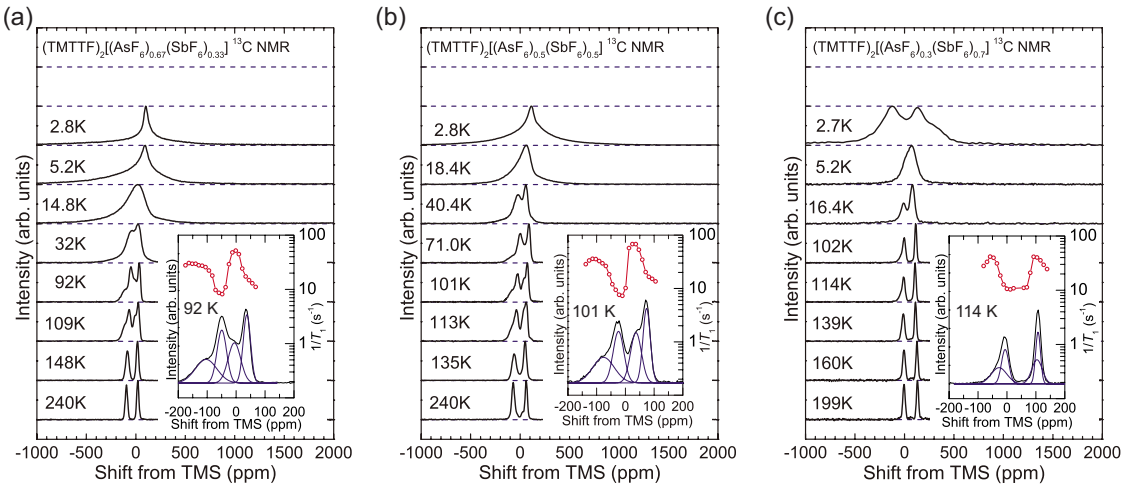

FIG. 1. (Color online) Temperature variation in ^{13}C NMR spectra of $(TMTTF)_2[(AsF_6)_x(SbF_6)_{1-x}]$ (a) $x\sim0.67$, (b) $x\sim0.5$, and (c) $x\sim0.3$. In each of the figures, the insets show the spectra at 92 K, 101 K, and 114 K below T_{CO} for $x\sim0.67$, 0.5, and 0.3, respectively. The spectra are decomposed into four Gaussian spectra. $1/T_1$ measured at discrete frequencies is plotted over each spectrum.

tiferromagnetic phase transition and the spin-gap transition are observed in the alloys with $x\sim0.3$ and 0.67, respectively. The present study suggests that the antiferromagnetic phase and spin-gap phase are in contact at low temperatures. The $x\sim0.5$ alloy is situated on the edge of the spin-gap phase, showing a gradual phase transition and significant critical fluctuations at low temperatures, which can be attributed to the quantum critical effect.

II. EXPERIMENTAL

^{13}C NMR measurements were performed for single crystals of $(TMTTF)_2[(AsF_6)_x(SbF_6)_{1-x}]$ $(x\sim0.3,0.5,0.67)$, whose double-bonded carbons at the center of the TMTTF molecule are ^{13}C enriched, in a temperature range from 2.7 to 270 K. An external magnetic field of ~8 T, which corresponds to an NMR frequency of 86.6 MHz, was applied perpendicular to the molecular stacking a axis. The magnetic field and the $^{13}C{=}{=}^{13}C$ vector form the so-called magic angle, $3\cos^2\theta-1=0$ $(\theta\sim55°)$, to vanish line splitting by nuclear dipolar coupling between the ^{13}C nuclei. The ^{13}C NMR spectra were obtained by Fourier transformation of the spin-echo signal refocused after $\pi/2$-π pulses. In this paper, we define the factor x as the ratio of the two different electrolyte salts used in the electrochemical preparation. It is reported that the factor x is close to ratio of electro supporting materials in the previous literatures.[10,12,25] We confirmed that T_{CO} and T_{AF} of $x\sim0.3$ are reasonable considering the previous data.

III. RESULTS AND DISCUSSION

The temperature variations in the ^{13}C NMR spectra of $(TMTTF)_2[(AsF_6)_x(SbF_6)_{1-x}]$ for $x\sim0.67$, $x\sim0.5$, and $x\sim0.3$ are shown in Figs. 1(a)–1(c), respectively. At high temperatures, two lines originating from two inequivalent ^{13}C sites in the TMTTF molecule are observed for the three salts. We label the line of the higher spectrum as line H and the lower one as line L. The spectra show broadening and become asymmetric with decreasing temperature due to the emergence of distinct ^{13}C sites. The CO transition is related to symmetry breaking of the inversion center in a unit cell that leads to four ^{13}C sites becoming inequivalent. The observation of four well-decomposed Gaussian spectra with the same intensity confirms the occurrence of the CO transition, as shown in the insets of Fig. 1 representing the typical split spectra for $x\sim0.67$ at 92 K, $x\sim0.5$ at 101 K, and $x\sim0.3$ at 114 K. The spin-lattice relaxation rate, $1/T_1$, is related to the charge quantity on the corresponding ^{13}C site. $1/T_1$ at discrete frequencies over the spectrum is shown in the insets of Fig. 1. $1/T_1$ is determined by fitting the nuclear recovery curve, which is the time dependence of the integrated signal intensity, fitted by a stretched exponential function $[M(\infty)-M(t)]/M(\infty)=\exp[-(t/T_1)^{\beta}]$, where β characterizes the distribution of $1/T_1$. The signal intensity is evaluated at intervals of 1 kHz by integrating the intensity of the spectrum within the range of 2 kHz. The signals from the charge-rich TMTTF molecules correspond to the spectra at the lower frequency side of line L and line H, whose $1/T_1$ is about ten times larger than that at the higher frequency side. The estimation of the charge separation amplitude, assuming $1/T_1$ is proportional to the square of the charge quantity, was not conducted here because the overlap of spectra prevents the precise estimation of $1/T_1$ for each spectrum. The possible origin of the poor resolution of the spectra is the effect of alloying. The spectra below T_{CO} are broader than those of the pure compounds while the line splitting of ~50 ppm is comparable to that of the pure compound $(TMTTF)_2AsF_6$.[9] The temperature dependence of the second moment of spectra, $\langle\Delta\omega^2\rangle$, is shown in Fig. 2. $\langle\Delta\omega^2\rangle$ decreases down to T_{CO} and increases again reflecting the line splitting below T_{CO}. The estimated T_{CO} is about 140 K, 125 K, and 120 K for $x=0.3$, 0.5, and 0.67, respectively, as denoted by the arrows in Fig. 2. β for Line H and L deviates from unity below T_{CO}, that supports the occurrence of the charge order. T_{CO} decreases with increasing amount of AsF_6. The reduction in T_{CO} by chemical pressure is consistent with the behavior observed for $(TMTTF)_2SbF_6$ and $(TMTTF)_2AsF_6$ under pressure.[16,19]

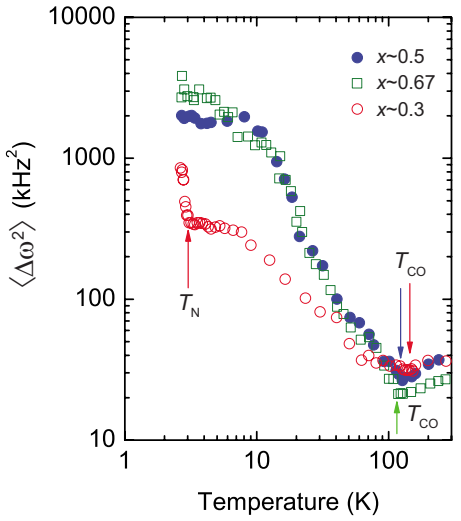

FIG. 2. (Color online) Temperature dependence of the second moment of the ^{13}C NMR spectra, $\langle\Delta\omega^2\rangle$. T_{CO} and T_N are indicated by arrows.

For $x\sim0.67$ and 0.5 the spectra exhibit further broadening below T_{CO}. This spectral broadening prevents the identification of peak positions of each spectrum below about 30 K. We plotted the temperature dependence of the peak positions of the spectra for $x\sim0.67$ and 0.5 in Figs. 3(a) and 3(b), respectively. The apparent slight shift to the higher frequency side of both peaks below T_{CO} comes from a sharp spectrum from the charge-poor site associated with the line splitting. Below about 15 K, the broad spectrum shifts to the higher frequency side for $x\sim0.67$. This behavior is consistent with the spin-singlet transition.[9,27] The decay in the spin density at the TMTTF molecules results in a reduction in the Knight shift. The detection of only one sharp spectrum at the lowest temperature measured supports the nonmagnetic ground state. Just above the spin-gap transition temperature, $T_{SG}\sim15$ K, the spectral shape of the $x\sim0.67$ salt indicates that

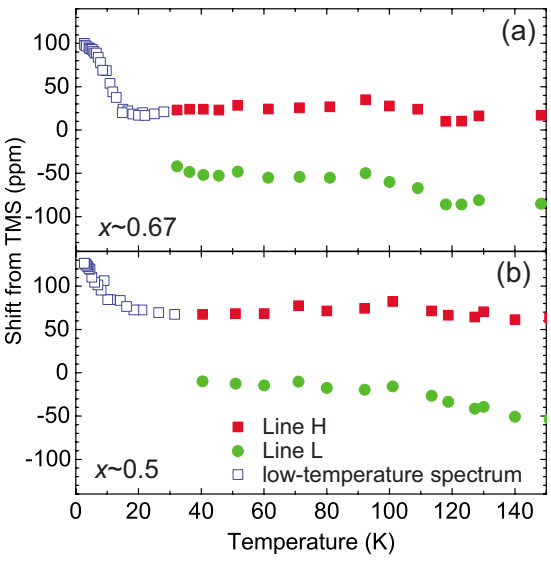

FIG. 3. (Color online) Temperature dependence of the peak position of the spectra of (a) $x\sim0.63$ and (b) $x\sim0.5$.

the spectrum consists of a diffusive broad spectrum in addition to the sharp one. The characteristic spectrum is observed in $(TMTTF)_2PF_6$ above $T_{SG}\sim18$ K and is attributed to the redistribution of the charge and/or spin as the precursor to the transition.[27] In the alloy of $x\sim0.5$, the spectral shift to the higher frequency side is also observed, as shown in Fig. 3(b), indicating that the ground state of this salt is also the spin-gap phase. However, the shift of the spectrum is small and gradual. Moreover, the linewidth remains broad at the lowest temperature. These results suggest that this compound is situated near the boundary of the spin-gap phase.

In the alloy of $x\sim0.3$, the spectral change is contrasting at low temperatures, showing symmetrical line splitting into two lines below about 2.9 K. This line splitting is reflected as a rapid increase in $\langle\Delta\omega^2\rangle$ as shown in Fig. 2. This behavior can be ascribed to an antiferromagnetic phase transition, in which the antiferromagnetic staggered moment produces two internal magnetic fields in the crystal. The Néel temperature of $T_N=2.9$ K is lower than $T_N=8$ K for the pure compound $(TMTTF)_2SbF_6$. The decrease in the Néel temperature by the introduction of AsF_6 agrees with the tendency already observed in alloys for low x.[25] In $(TMTTF)_2SbF_6$, the commensurate antiferromagnetic phase is suggested.[28] The alloy of $x\sim0.3$ is also expected to be commensurate in the ground state.

It is expected that the spin-lattice relaxation rate, $1/T_1$, increases when the characteristic frequency approaches the Larmor frequency (~MHz) at T_N, reflecting the critical slowing down of the spin fluctuations even if the frequency of the spin fluctuations does not reach the Larmor frequency. At high temperatures, away from T_N, $1/T_1$ is governed by the long-wavelength uniform component ($q\approx0$) of spin fluctuation, $(1/T_1)^{uniform}$.[29] If we assume a 1D electron-gas model,[29,30] the critical component, $(1/T_1)^{critical}$, becomes constant at $T_\rho>T\gg T_N$. In this temperature region, $(1/T_1)^{uniform}$ is written as $(1/T_1)^{uniform}\propto T\chi_s^2(T)$, where $\chi_s(T)$ is the static magnetic susceptibility. Consequently, the two components contribute to $1/T_1$ as $1/T_1=(1/T_1)^{critical}+(1/T_1)^{uniform}=C_1+C_0T\chi_s^2(T)$, where C_1 and C_0 are constant. Figure 4(a) shows the temperature dependence of $1/T_1$. Above about 100 K, $1/T_1$ decreases rapidly on cooling for the three salts. The temperature dependence of spin susceptibility χ_s is shown in Fig. 5. χ_s was determined by the integrated signal intensity of the ESR spectrum for a single crystal. Above about 30 K, χ_s gradually decreases with decreasing temperature. In Fig. 4(b), the behavior of $1/T_1$ as a function of $T\chi_s^2(T)$ for $x\sim0.5$ is shown. The data with the external field H_0 directed parallel to the molecular stacking direction ($H_0\|a$) are used in the analysis. $1/T_1$ shows the linear dependence on $T\chi_s^2(T)$ that confirms that the relaxation is determined by the 1D paramagnon magnetic excitations assumed in the above model. The temperature dependence of $1/(T_1T)$ is shown in the inset of Fig. 4(a). $1/(T_1T)$ above 100 K contrasts with the behavior of two-dimensional organic conductors $(BEDT\text{-}TTF)_2X$, where BEDT-TTF is bis(ethylenedithio)tetrathiafulvalene, in which $1/(T_1T)$ is almost temperature independent in the paramagnetic insulator region.[31] The 1D character of spin fluctuations is not affected by the disorder introduced by the alloying in the high-temperature region. The deviation from zero of $1/T_1$ when $T\chi_s^2\to0$, that

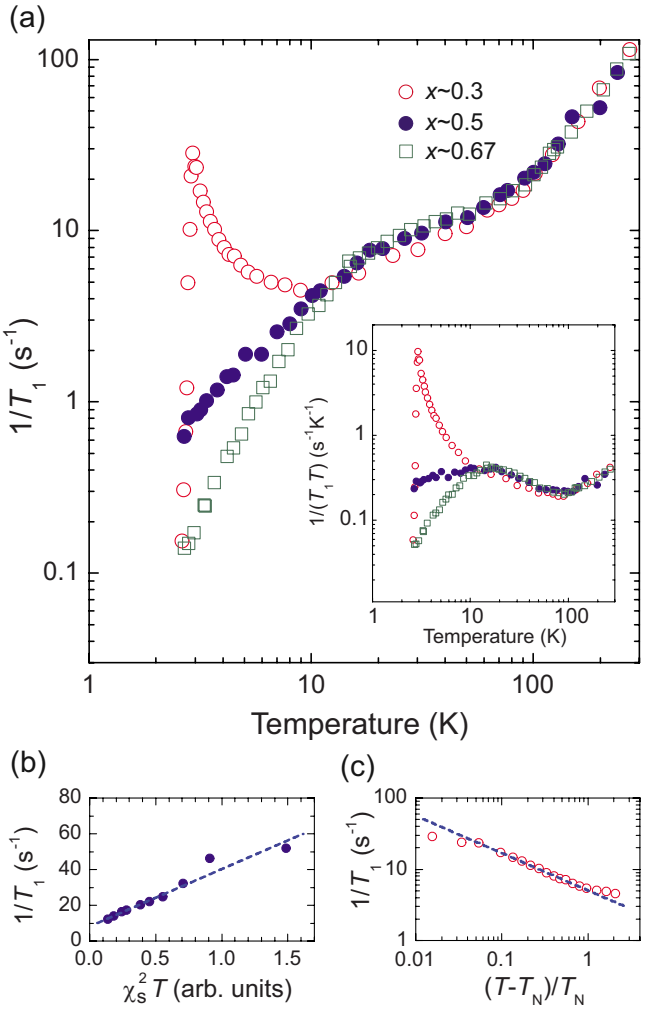

FIG. 4. (Color online) (a) Temperature dependence of $1/T_1$. The inset shows the temperature dependence of $1/(T_1T)$. (b) $1/T_1$ as a function of $\chi_s^2 T$ for the alloy of $x \sim 0.5$. (c) Power-law behavior of $1/T_1$ for the alloy of $x \sim 0.3$ on approaching T_N by lowering temperature.

is $C_1 \neq 0$, indicates the existence of the critical contribution $(1/T_1)^{\text{critical}}$, which is associated with the enhancement of $1/(T_1T)$ below 100 K.

Below about 100 K, $1/(T_1T)$ increases with decreasing temperature. In the salt of $x \sim 0.3$, $1/T_1$ shows a rapid increase on approaching $T_N = 2.9$ K due to the critical slowing down of the antiferromagnetic spin fluctuations. $1/T_1$ drops rapidly below T_N as a result of the disappearance of the critical fluctuations in the ordered state. The singular behavior around the phase-transition point is characterized by the power-law dependence of the physical quantities. In particular, $1/T_1$ characterizes the dynamical property of the phase transition.[32] In Fig. 4(c), $1/T_1$ is plotted as a function of the reduced temperature $r=(T-T_N)/T_N$ above T_N. $1/T_1$ is well described by the power law, $1/T_1 \propto r^{\gamma}$, for $0.05 < r < 0.8$. We obtained the critical exponent $\gamma = 0.5$ by fitting the relation. The theoretical study predicts $\gamma = 0.5$,[30] which is also the case for the three-dimensional system.[32] A similar value is obtained in $(TMTTF)_2Br$ and $(TMTTF)_2PF_6$ under 13 kbar, whose ground state is the antiferromagnetic state.[33] The exponent is apparently robust over the CO transition and alloy disorder. The width of the critical region defined by $\Delta t_{\text{fl}} \equiv (T_{\text{fl}} - T_N)/T_N$ provides another feature of the phase transition, where T_{fl} is the temperature below which $1/T_1$ shows the upward curvature. We found $T_{\text{fl}} = 9$ K for this salt that yields $\Delta t_{\text{fl}} \simeq 2$ which is fairly larger than $\Delta t_{\text{fl}} \simeq 0.6$ for the case of $(TMTTF)_2Br$ and $(TMTTF)_2PF_6$.[33] This deviation suggests there is another mechanism which induces the spin-lattice relaxation above T_N. If the interchain coupling is weak in this alloy system, one-dimensional correlation should enhance the antiferromagnetic fluctuations. Another possibility is the quantum critical effect. The quantum critical effect for the continuous phase transition, if any, will be emphasized at such low temperatures because the (classical) critical region becomes narrow depending on the scaling relation.[23] In fact, the critical temperature of $T_N = 2.9$ K is relatively low.

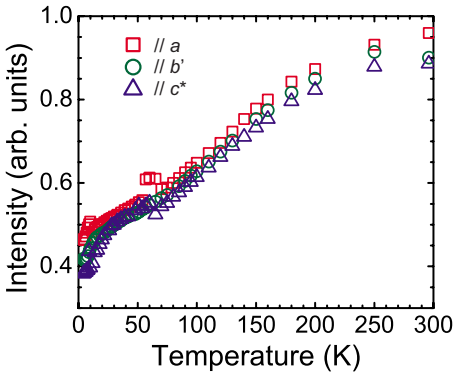

FIG. 5. (Color online) Temperature dependence of spin susceptibility, χ_s, for the alloy of $x \sim 0.5$.

In the alloys of $x \sim 0.5$ and 0.67, the decrease in $1/T_1$ becomes slower below about 100 K, even though the ground state is not antiferromagnetic. This behavior is not associated with the charge ordering because T_{CO} deviates slightly from the anomalous temperature. The similar behavior with $x \sim 0.3$ infers that the origin is the antiferromagnetic correlation as discussed above. $1/T_1$ of $x \sim 0.67$ drops rapidly without the increase below about 15 K that indicates the opening of the spin gap. This behavior confirms the spin-singlet transition reflected in the line shift. The decrease in $1/T_1$ of the alloy of $x \sim 0.5$, in contrast, is very weak. $1/(T_1T)$ is almost temperature independent. This behavior and the observation of the gradual NMR shift indicate that this salt is located in the vicinity of the low end of the spin-gap phase. The considerable relaxation rate at low temperature can be ascribed to the critical spin fluctuations. As the antiferromagnetic phase and the spin-gap phase presumably share a boundary at very low temperatures, the $1/T_1$ of the salt of $x \sim 0.5$ possibly detects antiferromagnetic spin fluctuations. The power of the stretched exponential function, β, of $x \sim 0.5$ decreases to 0.5 at low temperatures, indicating that the distribution of $1/T_1$ is large. This is interpreted as enhancement of phase inhomogeneity on approaching the quantum critical point, which is the phase-transition point at absolute zero temperature.[34] For $x \sim 0.3$ and 0.63, in contrast, β increases again below T_{AF} and T_{SG}.

The *P-T* phase diagram of this alloy system is illustrated in Fig. 6. The previously reported resistivity measurement

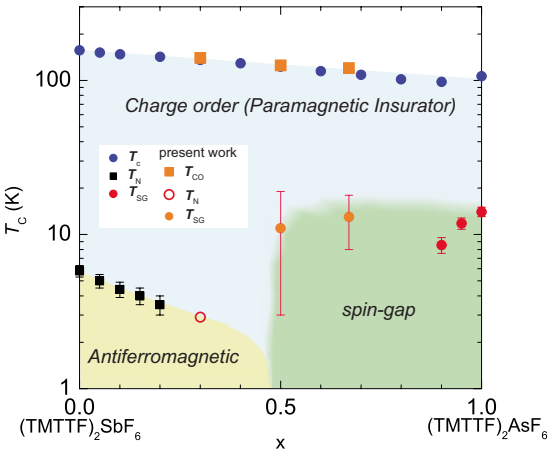

FIG. 6. (Color online) The phase diagram of the $(TMTTF)_2[(AsF_6)_x(SbF_6)_{1-x}]$ alloy system. The previous data of T_c, T_N, and T_{SG} near the pure compounds are also plotted in the figure (Refs. 12 and 25).

showed that T_c, defined as the maximum temperature of $d[\ln \rho]/d(1/T)$, decreases with the concentration of AsF_6.[12] The charge-ordering temperature, T_{CO}, determined by the NMR measurement in this work shows the same tendency, which confirms the assumption of $T_c=T_{CO}$.[14] The critical temperature of the antiferromagnetic phase transition, T_N, for $x\sim0.3$ is well defined by the NMR line splitting and the pronounced peak in $1/T_1$. The decrease in T_N with the concentration of AsF_6 corroborates the behavior observed by ESR in the previous report.[25,26] The spin-gap transition for the salt, whose concentration x is greater than 0.5, is continuous. The salt of $x\sim0.5$ is located near the boundary of the spin-gap phase. The reduction in T_{SG} in the intermediate pressure range observed in the salts near $(TMTTF)_2AsF_6$ is not obvious in this study.[25] The magnetic field effect is an important issue in the one-dimensional system. For instance, $(TMTTF)_2PF_6$ shows an incommensurate phase above about 19.1 T.[35] In the spin-gap phase, the estimate of the magnitude of the spin gap can be affected by the magnetic field. The magnetic field of 8 T applied in this experiment, however, is too small to induce the incommensurate spin-gap phase in this system. We have not detected the effect on the critical temperatures T_{SG} and T_{AF}. For TMTTF salts, field-induced magnetic phases has not been observed so far, and might be stabilized only under very high field.

IV. CONCLUSION

We carried out ^{13}C NMR measurements on the alloy system $TMTTF_2[(AsF_6)_x(SbF_6)_{1-x}]$ $(x\sim0.3,0.5,0.67)$ in order to understand the physical properties around the phase boundary between the antiferromagnetic phase and the spin-gap phase. The observation of line splitting indicates the occurrence of the CO transition. The antiferromagnetic phase transition and spin-gap phase transition are observed in the alloys $TMTTF_2[(AsF_6)_{0.3}(SbF_6)_{0.7}]$ and $TMTTF_2[(AsF_6)_{0.67}(SbF_6)_{0.33}]$, respectively. The quasi-1D correlation and antiferromagnetic critical behavior are discussed in terms of the power-law behavior of $1/T_1$. For $TMTTF_2[(AsF_6)_{0.5}(SbF_6)_{0.5}]$, the NMR shift and the depression of $1/T_1$ are weak compared to the spin-gap transition material, indicating that this salt is situated near the phase boundary between the antiferromagnetic and spin-gap phases. Our measurements demonstrate that $1/T_1$ shows anomalous behavior in the quantum critical regime near the boundary of both phases at low temperatures. The phase diagram of the alloy system is proposed.

ACKNOWLEDGMENTS

The authors wish to thank H. Seo, M. Itoi, K. Yonemitsu, P. Monceau, T. Takahashi, and H. Fukuyama for discussions. This study was supported by a Grant-in-Aid for Scientific Research (B) under Grant No. 20340095 from JSPS, Scientific Research on Innovative Areas (Grant No. 21110523) from MEXT. F.I. was partially supported by Yazaki Memorial Foundation for Science and Technology. K.F. was partially supported by a Grant-in-Aid Areas (Grant No. 21110523) and for Young Scientists (A) (Grant No. 21685021) from JSPS.

*Present address: Department of Physics, Okayama University, Okayama 700-8530, Japan.

[1] D. Jérome, Science **252**, 1509 (1991).
[2] T. Ishiguro, K. Yamaji, and G. Saito, *Organic Superconductors*, 2nd ed. (Springer, Berlin, Tokyo, 1998).
[3] N. Toyota, M. Lang, and J. Mueller, *Low-Dimensional Molecular Metals* (Springer, Berlin, 2007).
[4] F. Iwase, K. Sugiura, K. Furukawa, and T. Nakamura, J. Phys. Soc. Jpn. **78**, 104717 (2009).
[5] M. Itoi, C. Araki, M. Hedo, Y. Uwatoko, and T. Nakamura, J. Phys. Soc. Jpn. **77**, 023701 (2008).
[6] A. Maaroufi, S. Flandrois, G. Fillion, and J. P. Morand, Mol. Cryst. Liq. Cryst. **119**, 311 (1985).
[7] C. Coulon, J. C. Scott, and R. Laversanne, Mol. Cryst. Liq. Cryst. **119**, 307 (1985).
[8] M. Dumm, B. Salameh, M. Abaker, L. K. Montgomery, and M. Dressel, J. Phys. IV **114**, 57 (2004).
[9] S. Fujiyama and T. Nakamura, J. Phys. Soc. Jpn. **75**, 014705 (2006).
[10] R. Laversanne, J. Amiell, C. Coulon, C. Garrigou-Lagrange, and P. Delhaes, Mol. Cryst. Liq. Cryst. **119**, 317 (1985).
[11] M. de Souza, A. Bruhl, J. Muller, P. Foury-Leylekian, A. Moradpour, J.-P. Pouget, and M. Lang, Physica B **404**, 494 (2009).
[12] R. Laversanne, C. Coulon, B. Gallois, J. P. Pouget, and R. Moret, J. Phys. (France) Lett. **45**, L393 (1984).
[13] M. Itoi, M. Kano, N. Kurita, M. Hedo, Y. Uwatoko, and T. Nakamura, J. Phys. Soc. Jpn. **76**, 053703 (2007).
[14] M. Nagasawa, T. Nagasawa, K. Ichimura, and K. Nomura, J. Phys. Soc. Jpn. **77**, 105002 (2008).
[15] D. S. Chow, F. Zamborszky, B. Alavi, D. J. Tantillo, A. Baur, C.

A. Merlic, and S. E. Brown, Phys. Rev. Lett. **85**, 1698 (2000).
[16] F. Zamborszky, W. Yu, W. Raas, S. E. Brown, B. Alavi, C. A. Merlic, and A. Baur, Phys. Rev. B **66**, 081103(R) (2002).
[17] K. Furukawa, T. Hara, and T. Nakamura, J. Phys. Soc. Jpn. **74**, 3288 (2005).
[18] W. Yu, F. Zamborszky, B. Alavi, A. Baur, C. A. Merlic, and S. E. Brown, J. Phys. IV **114**, 35 (2004).
[19] W. Yu, F. Zhang, F. Zamborszky, B. Alavi, A. Baur, C. A. Merlic, and S. E. Brown, Phys. Rev. B **70**, 121101(R) (2004).
[20] S. Sachdev, Rev. Mod. Phys. **75**, 913 (2003).
[21] S. Sachdev, Science **288**, 475 (2000).
[22] S. L. Sondhi, S. M. Girvin, J. P. Carini, and D. Shahar, Rev. Mod. Phys. **69**, 315 (1997).
[23] M. Vojta, Rep. Prog. Phys. **66**, 2069 (2003).
[24] G. R. Stewart, Rev. Mod. Phys. **73**, 797 (2001).
[25] R. Laversanne, J. Amiell, and C. Coulon, Mol. Cryst. Liq. Cryst. **137**, 169 (1986).
[26] T. Nakamura and K. Maeda, J. Phys. IV **114**, 123 (2004).
[27] T. Nakamura, K. Furukawa, and T. Hara, J. Phys. Soc. Jpn. **76**, 064715 (2007).
[28] T. Nakamura, F. Iwase, H. Satsukawa, K. Furukawa, and T. Takahashi, J. Phys.: Conf. Ser. **150**, 042137 (2009).
[29] C. Bourbonnais, P. Wzietek, F. Creuzet, D. Jérome, P. Batail, and K. Bechgaard, Phys. Rev. Lett. **62**, 1532 (1989).
[30] C. Bourbonnais, J. Phys. I **3**, 143 (1993).
[31] A. Kawamoto, K. Miyagawa, Y. Nakazawa, and K. Kanoda, Phys. Rev. B **52**, 15522 (1995).
[32] P. C. Hohenberg and B. I. Halperin, Rev. Mod. Phys. **49**, 435 (1977).
[33] P. Wzietek, F. Creuzet, C. Bourbonnais, D. Jérome, K. Bechgaard, and P. Batail, J. Phys. I **3**, 171 (1993).
[34] F. Iwase, K. Sugiura, K. Furukawa, and T. Nakamura, J. Phys.: Conf. Ser. **132**, 012015 (2008).
[35] S. E. Brown, W. G. Clark, F. Zamborszky, B. J. Klemme, G. Kriza, B. Alavi, C. Merlic, P. Kuhns, and W. Moulton, Phys. Rev. Lett. **80**, 5429 (1998).